# Open Research Online

The Open University's repository of research publications
and other research outputs

# Fast EM principal component analysis image registration using neighbourhood pixel connectivity

## Conference or Workshop Item

How to cite:

Reel, Parminder Singh; Dooley, Laurence S.; Wong, K. C. P. and Börner, Anko (2013). Fast EM principal component analysis image registration using neighbourhood pixel connectivity. In: 15th International Conference on Computer Analysis of Images and Patterns, 27-29 Aug 2013, York.

For guidance on citations see FAQs.

# oro.open.ac.uk

# Fast EM Principal Component Analysis Image Registration using Neighbourhood Pixel Connectivity

Parminder Singh Reel[1], Laurence S. Dooley[1], K. C. P. Wong[1], and A. Börner[2]

[1] Department of Communication and Systems, The Open University, Milton Keynes, United Kingdom
{p.s.reel, laurence.dooley, k.c.p.wong}@open.ac.uk,
[2] Optical Sensor Systems, German Aerospace Center (DLR), Berlin, Germany
anko.boerner@dlr.de

**Abstract.** *Image registration* (IR) is the systematic process of aligning two images of the same or different modalities. The registration of mono and multimodal images i.e., magnetic resonance images, pose a particular challenge due to *intensity non-uniformities* (INU) and noise artefacts. Recent similarity measures including *regional mutual information* (RMI) and *expectation maximisation for principal component analysis* with *MI* (EMPCA-MI) have sought to address this problem. EMPCA-MI incorporates neighbourhood region information to iteratively compute principal components giving superior IR performance compared with RMI, though it is not always effective in the presence of high INU. This paper presents a *modified* EMPCA-MI (*m*EMPCA-MI) similarity measure which introduces a novel pre-processing step to exploit local spatial information using 4-and 8-pixel neighbourhood connectivity. Experimental results using diverse image datasets, conclusively demonstrate the improved IR robustness of *m*EMPCA-MI when adopting second-order neighbourhood representations. Furthermore, *m*EMPCA-MI with 4-pixel connectivity is notably more computationally efficient than EMPCA-MI.

**Keywords:** Image registration, mutual information, principal component analysis, expectation maximisation algorithms.

## 1   Introduction

*Image Registration* (IR) is a vital processing task in numerous applications where the final information is obtained by combining different data sources, as for example in computer vision, remote sensing and medical imaging [14]. The process of IR involves the geometric transformation of a source image in order to attain the best physical alignment with a reference target image. It applies an optimization method to maximize some predefined similarity measure with known transformations between the source and reference image set.

Similarity measures which have been proposed [14] for both mono and multimodal IR can be broadly categorized according to whether they are based on

cross correlation, phase correlation, Fourier techniques or *mutual information* (MI) [4], with MI being well-established in the medical imaging domain [1]. MI is computationally efficient and seeks to form a statistical relationship between the source and reference images [12]. It is however, sensitive to interpolation artefacts and its performance can be severely compromised when the overlap region between the images is small.

Normalized MI (NMI) [11] was specifically designed to facilitate the sucessful IR of partially overlapping images, though it along with MI is unable to consistently and accurately register images containing *intensity non-uniformities* (INU) [10] which is an omnipresent feature in *magnetic resonance images* (MRI) for instance. In contrast, regional MI (RMI) [9] and its variant [13] incorporate neighbourhood features within MI by segmenting an image into several regions for feature extraction to lessen the influence of INU on the resulting IR quality. In computing the associated entropies, these MI-based approaches employ a covariance matrix instead of high-dimensional histograms to reduce data complexity, though as the size of a neighbourhood region grows, so the computation overheads commensurately increase [9].

The *expectation maximisation for principal component analysis* with *MI* (EM PCA-MI) algorithm [7] is a recently proposed IR similarity measure, which significantly reduces the computational cost without loss of IR performance for different mono and multimodalities of the human anatomy [6],[5]. Its performance however, can be compromised in the presence of high INU and noise levels [7]. EMPCA-MI achieves dimensionality reduction by iteratively determining the principal component without recourse to solving the complete covariance matrix as in conventional *principal component analysis* (PCA) techniques. As a pre-processing step, EMPCA-MI rearranges the neighbourhood region grayscale data values into vector form so preserving both the spatial and intensity information of the images.

This paper presents a *modified* EMPCA-MI (*m*EMPCA-MI) similarity measure which uses the difference in grayscale values for direct (*4-pixel*) and indirect (*8-pixel*) neighbourhood relations, instead of rearranging the pixels in the pre-processing stage. This provides the dual advantages of more accurate feature representation for EMPCA and MI computation, and significantly lower computational cost with, as will be evidenced in Section 4, minimal impact upon the corresponding IR performance compared with EMPCA-MI. Quantitative results verify the new pre-processing step adopted in *m*EMPCA-MI provides superior IR performance from both a registration error and computational time perspective for various mono and multimodal test datasets. The remainder of the paper is organized as follows: Section 2 briefly reviews the original EMPCA-MI similarity measure before the proposed *m*EMPCA-MI pre-processing step exploiting localised pixel relations is introduced. Section 3 describes the experimental test setup used, while Section 4 presents an IR results analysis of the *m*EMPCA-MI algorithm. Finally, Section 5 provides some concluding comments.

## 2    The $m$EMPCA-MI Model

### 2.1    EMPCA-MI Similarity Measure [7]

EMPCA-MI [7] is a recent similarity measure for IR, which efficiently incorporates spatial information together with MI without incurring high computational overheads. Fig. 1 illustrates the three core processing steps involved in the EMPCA-MI algorithm, namely: input image data rearrangement (highlighted in *yellow*) followed by EMPCA and MI calculation. Both the reference ($I_R$) and source images ($I_S$) are pre-processed (*Step I*) into vector form for a given neighbourhood radius $r$, so the spatial and intensity information is preserved (see Fig. 1(a) and 1(b)). The first $P$ principal components $X_R$ and $X_S$ of the respective reference and source images are then iteratively computed using EMPCA [8] in *Step II*. Subsequently, the MI [1] is calculated between $X_R$ and $X_S$ in *Step III*, with a higher MI value signifying the images are better aligned. In [7], only the first principal component is considered, i.e., *P=1* since this is the direction of highest variance and represents the most dominant feature in any region.

### 2.2    New Pre-processing Step

As evidenced in Fig. 1(a), *Step I* of the EMPCA-MI algorithm reorganises the image grayscale values within each neighbourhood region in order to incorporate spatial information. This provides noteworthy IR results [7] when there is neither INU nor noise present, however when there are high levels of INU and noise, the corresponding registration performance can degrade because only a first-order region representation is used which considers each pixel independently without cognisance of any neighbourhood relations. This is reflected in the repetitive patterns in $Q_R$ and $Q_S$ in the neighbouring position of the sliding window (See *Step I*(b) in Fig 1). The rationale behind the proposed $m$EMPCA-MI pre-processing step is that spatial information within a neighbourhood region can be more accurately characterised as second-order representation, where the relationship between pixels can be exploited instead of just pixel values. To illustrate the new pre-processing step for $m$EMPCA-MI, consider the example shown in Fig. 1, for a *3* x *3* pixel sliding window (*r=1*) neighbourhood region $B$ (see Fig. 1(a)) which assumes either *4-pixel* (direct neighbours) or *8-pixel* (indirect neighbours) connectivity i.e., *c=4* and *c=8* respectively. The resulting single column vector $B^*$ will thus have length *c+1* as shown in Fig. 1(b), and can be represented as:

$$B_i^* = \begin{cases} B_i - B_5 & i \in [1, c+1]; i \notin [5] \\ B_5 & i \in [5] \end{cases} \tag{1}$$

Each column vector $B^*$ now represents the differential value of $c$ connected pixels with respect to the centre pixel $B_5$. Here, $m$EMPCA-MI pre-processing no longer generates repetitive pattern as in EMPCA-MI, but instead provides unique relative intensity values (See $B^*$ in Fig.1) for the next computational steps in the $m$EMPCA-MI.
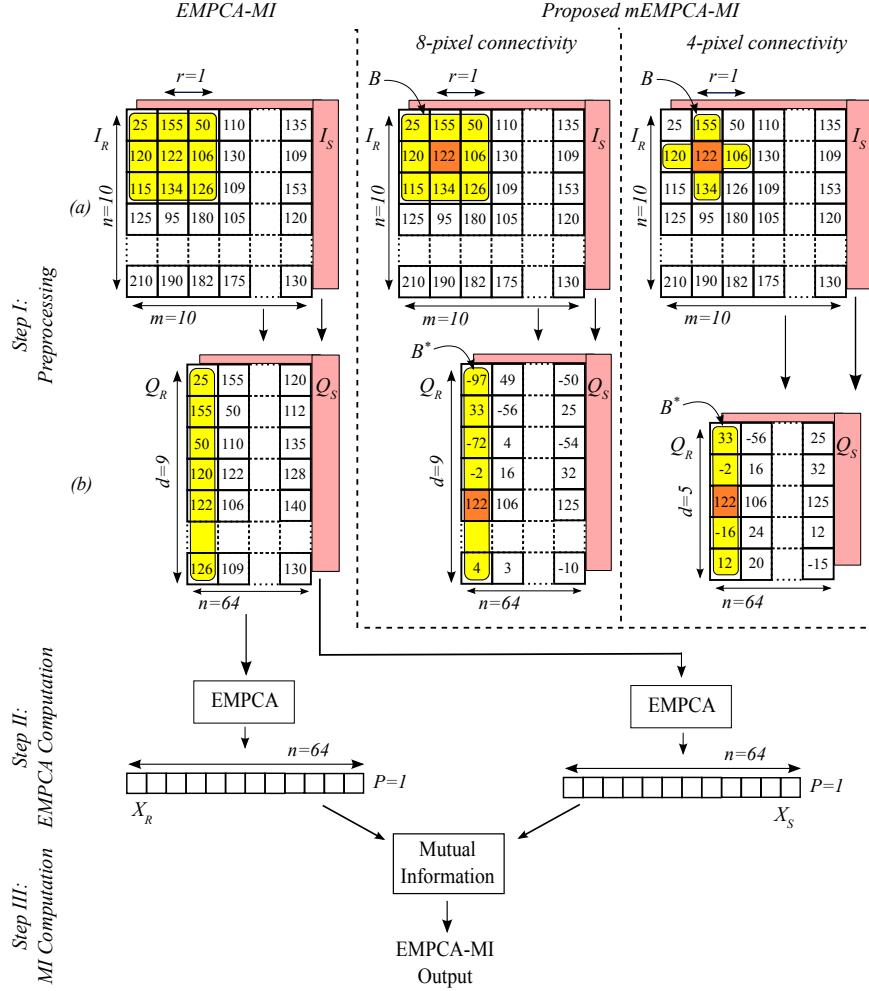
**Fig. 1.** Illustration of the EMPCA-MI algorithm [7], together with the proposed *m*EMPCA-MI pre-processing step using neighbourhood 8-pixel and 4-pixel region connectivity for an image pair size of *10* x *10* pixels.

Once *Step I* has been completed, the remaining two processing steps of *m*EMPCA-MI are as in [7]. Fig 2. displays two *m*EMPCA-MI traces for both 4-pixel and 8-pixel connectivity together with EMPCA-MI with respect to the $\theta$ angular rotational transformation parameter for the IR of the multimodal MRI pair T1 and T2. Fig 2(a) shows IR case when there is neither INU nor noise present, while Fig 2(b) reflects the challenging registration of 40% INU and Gaussian noise. It is palpable the *m*EMPCA-MI traces for both 4-pixel and 8-pixel neighbourhood connectivity provide smoother and higher similarity measure values for the best alignment compared with EMPCA-MI.
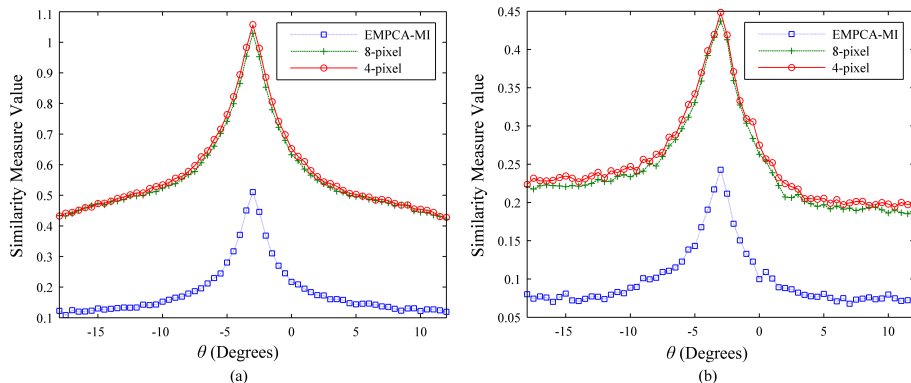
**Fig. 2.** Similarity measure value traces for EMPCA-MI and $m$EMPCA-MI (8-pixel and 4-pixel connectivity). (a) shows the angular rotation transformation for MRI T1 and T2 multimodal registration (without INU and noise) and (b) with 40% INU and noise.

Interestingly 4-pixel neighbourhoods are better in both cases, since they exploit the neighbourhood relations with the strongest links leading to a correspondingly higher overall MI value between $I_R$ and $I_S$. Fig 2 also highlights the smooth convergence of $m$EMPCA-MI compared with EMPCA-MI with less oscillatory behaviour particularly where 40% INU and noise is present. This is a very useful feature for effective convergence of the ensuing optimization process [14] and ultimately leads to lower IR errors.

## 3   Experiment Setup

To evaluate the performance of the $m$EMPCA-MI similarity measure, a series of multimodal IR experiments were undertaken. Multimodal MRI T1 and T2 datasets from BrainWeb Database [2] were chosen due to their challenging characteristics of varying INU and noise artefacts with the corresponding parameter details being defined in Table 1. To simulate a range of applications and analyse the robustness of $m$EMPCA-MI, both *Lena* and *Baboon* images have also been used with a simulated INU function $Z$ [3]. Finally, Gaussian noise has been added to all the datasets. The IR experiments were classified into four separate scenarios representing monomodal, multimodal and two generic registrations.

**Table 1.** Dataset Parameter Details

| Dataset | Resolution (pixels) | INU | Noise($\beta$) |
|---------|---------------------|-----|----------------|
| MRI T1 (T1) | [181 x 217 x 181] | $\alpha_{20}$=20% INU | Gaussian |
| MRI T2 (T2) | [181 x 217 x 181] | $\alpha_{40}$=40% INU | ($\mu$=0.01, |
| *Lena* (L) | [256 x 256] | $Z$(x,y)=$\frac{1}{3.2}(x+y)$ [3] | $\sigma^2$=0.01) |
| *Baboon* (Bb) | [256 x 256] | | |

**Table 2.** Registration Error Results for Different *Scenarios*

| *Scenario* No. | $I_R$ | $I_S$ | EMPCA-MI [6] ($r=1,P=1$)) $\Delta X,\ \Delta Y,\ \Delta\theta$ (%) | *m*EMPCA-MI ($r=1,P=1$) 8-pixel $\Delta X,\ \Delta Y,\ \Delta\theta$ (%) | 4-pixel $\Delta X,\ \Delta Y,\ \Delta\theta$ (%) |
|---|---|---|---|---|---|
| 1 | T1+$\alpha_{20}$ | T1 | 2.0, 1.3, 0.36 | 1.26, 0.98, 0.24 | 1.12. 0.93, 0.21 |
|  | T1+$\alpha_{40}$ |  | 4.5, 4.0, 0.42 | 3.05, 3.21, 0.39 | 2.96, 3.04, 0.32 |
|  | T1+$\beta$ |  | 6.0, 7.0, 0.52 | 5.74, 6.58, 0.45 | 5.41, 6.25, 0.43 |
|  | T1+$\alpha_{40}+\beta$ |  | 8.0, 10.0, 0.58 | 7.84, 9.59, 0.48 | 7.45, 9.28, 0.46 |
| 2 | T1+$\alpha_{20}$ | T2 | 2.6, 2.6, 0.42 | 2.05, 1.98, 0.36 | 1.93, 1.71, 0.32 |
|  | T1+$\alpha_{40}$ |  | 4.8, 4.6, 0.62 | 4.12, 4.27, 0.48 | 3.98, 4.10, 0.43 |
|  | T1+$\beta$ |  | 6.2, 3.0, 0.46 | 5.82, 2.32, 0.37 | 5.68, 2.18, 0.33 |
|  | T1+$\alpha_{40}+\beta$ |  | 9.7, 4.3, 0.62 | 9.12, 3.28, 0.58 | 8.99, 3.11, 0.56 |
| 3 | L+$Z$ | L | 0.2, 0.32, 0.21 | 0.18, 0.28, 0.19 | 0.16, 0.24, 0.17 |
|  | L+$\beta$ |  | 0.32, 0.50, 0.36 | 0.29, 0.47, 0.31 | 0.27, 0.45, 0.29 |
|  | L+$Z$+$\beta$ |  | 2.0, 5.33, 0.21 | 1.95, 5.28, 0.20 | 1.93, 5.26, 0.19 |
| 4 | Bb+$Z$ | Bb | 0.45, 0.70, 0.21 | 0.32, 0.63, 0.18 | 0.30, 0.60, 0.16 |
|  | Bb+$\beta$ |  | 0.8, 1.26, 0.21 | 0.71, 1.14, 0.19 | 0.69, 1.12, 0.18 |
|  | Bb+$Z$+$\beta$ |  | 1.4, 1.50, 0.23 | 1.27, 1.24, 0.22 | 1.20, 1.22, 0.20 |

Each experiment involved an initial misregistration of predefined $x$ and $y$ axis translations and rotation $\theta$. The registration process involved partial volume interpolation along with Powell optimization method [4] to iteratively estimate the transformation parameters. The parameter values at which the *m*EMPCA-MI similarity measure is a maximum then define the final transformation for which the two images are best aligned. The registration error is defined as the difference between the initial and final value for each parameter. All experiments were performed upon an Ubuntu 10.04 (lucid) with 2.93 GHz Intel Core and 3GB RAM, and the assorted algorithms implemented in MATLAB.

## 4   Results Discussion

Table 2 shows the IR error results for all four *Scenarios* in terms of the percentage translation ($\Delta X$, $\Delta Y$) and angular rotational ($\Delta\theta$) errors. To clarify the nomenclature adopted in Table 2; T1+$\alpha_{20}$ for example, represents an MRI T1 image slice with 20% INU, while Bb+$Z$+$\beta$ refers to the *Baboon* image with INU and Gaussian noise artefacts. The results confirm the *m*EMPCA-MI algorithm using both 8-pixel and 4-pixel neighbourhood connectivity consistently provides better registration than the EMPCA-MI model for both mono and multimodal MRI T1 and T2 images, both when there is and is not INU and noise present.

For example, in monomodal IR *Scenario 1* with 40% INU and noise present (T1+$\alpha_{40}$+$\beta$), 8-pixel and 4-pixel connectivity *m*EMPCA-MI provide percentage errors for the ($\Delta X$, $\Delta Y$, $\Delta\theta$) parameters of (*7.84, 9.59, 0.48*) and (*7.45, 9.28, 0.46*) respectively which are both lower than the corresponding EMPCA-MI error (*8.0, 10.0, 0.58*). Similar performance improvements are also evident for *Lena* and *Baboon* images.

**Table 3.** Average Runtimes ($ART$) Results (in $ms$) for Different *Scenarios*

| *Scenario* *No.* | EMPCA-MI [6] $(r=1,P=1)$) | *m*EMPCA-MI ($r=1,P=1$) | |
|---|---|---|---|
| | | 8-pixel | 4-pixel |
| 1 2 | 152 | 144 | 95 |
| 3 4 | 170 | 156 | 109 |

This corroborates the fact that the *m*EMPCA-MI algorithm using both 8-pixel and 4-pixel connectivity in the pre-processing step more accurately reflects neighbourhood spatial information by considering a second-order representation of region pixels values with respect to centre pixel of the sliding window. The results also reveal that the IR error performance of *m*EMPCA-MI with 4-pixel neighbourhood connectivity is consistently lower than 8-pixel connectivity across all four *Scenarios*. Particularly striking, is the performance achieved for the challenging MRI T1 and T2 multimodal registration in *Scenario 2*, in the presence of both INU and noise. This reflects that 4-pixel neighbourhood connectivity exploits the direct pixel relations providing more relevant spatial information about local neighbourhood for subsequent EMPCA and MI computation. In contrast, 8-pixel connectivity also considers weaker indirect neighbours, which marginally reduces the corresponding principal component values leading to a lower MI between the image pair.

Table 3 displays the *average runtimes* ($ART$) for both EMPCA-MI and *m*EMPCA-MI. While $ART$ is a resource dependent metric, it concomitantly provides an insightful time complexity comparator between similarity measures. As illustrated in Fig. 1, since the data dimensionality of *m*EMPCA-MI with 4-pixel connectivity is reduced to 5 from 9 for both 8-pixel connectivity and EMPCA-MI [8], the corresponding $ART$ values are considerably lower, i.e., *95ms* compared to *144ms* for 8-pixel connectivity and *152ms* for EMPCA-MI to determine only the first principal component for *Scenarios 1* and *2*. A similar trend in the $ART$ values is observed in *Scenarios 3* and *4*, though these datasets have a different spatial resolution compared to *Scenarios 1* and *2*. Overall, the $ART$ results reveal a notable improvement in computational efficiency for *m*EMPCA-MI using 4-pixel neighbourhood connectivity, allied with superior IR robustness to both INU and noise for both mono and multimodal image datasets.

## 5   Conclusion

This paper has presented a neighbourhood connectivity based modification to the existing *Expectation Maximisation for Principal Component Analysis* with *MI* (EMPCA-MI) similarity measure. Superior and enhanced robust image registration performance in the presence of both INU and Gaussian noise has been achieved by incorporating second-order neighbourhood region information

compared with the grayscale value rearrangement in the original EMPCA-MI paradigm. Additionally, the 4-pixel connectivity $m$EMPCA-MI similarity measure is computationally more efficient compared to both EMPCA-MI and using 8-pixel neighbourhood connectivity.

## References

1. Collignon, Maes, F., Delaere, D., Vandermeulen, D., Suetens, P., Marchal, G.: Automated multi-modality image registration based on information theory. Imaging 3(1), 263–274 (1995)
2. Collins, D.L., Zijdenbos, A.P., Kollokian, V., Sled, J.G., Kabani, N.J., Holmes, C.J., Evans, A.C.: Design and construction of a realistic digital brain phantom. IEEE Transactions on Medical Imaging 17(3), 463–468 (Jun 1998)
3. Garcia-Arteaga, J.D., Kybic, J.: Regional image similarity criteria based on the kozachenko-leonenko entropy estimator. In: IEEE Computer Society Conference on Computer Vision and Pattern Recognition Workshops, 2008. CVPRW '08. pp. 1–8. IEEE (Jun 2008)
4. Pluim, J., Maintz, J., Viergever, M.: Mutual-information-based registration of medical images: a survey. IEEE Transactions on Medical Imaging 22(8), 986–1004 (Aug 2003)
5. Reel, P., Dooley, L., Wong, P., Börner, A.: Robust retinal image registration using expectation maximisation with mutual information. In: 38th IEEE International Conference on Acoustics, Speech, and Signal Processing (ICASSP 2013), IEEE, 2013. pp. 1118–1122. Vancouver, Canada (May 2013)
6. Reel, P.S., Dooley, L.S., Wong, K.C.P.: Efficient image registration using fast principal component analysis. In: 19th IEEE International Conference on Image Processing (ICIP 2012), IEEE, 2012. pp. 1661–1664. Lake Buena Vista, Orlando, Florida, USA (Sep 2012)
7. Reel, P.S., Dooley, L.S., Wong, K.C.P.: A new mutual information based similarity measure for medical image registration. In: IET Conference on Image Processing (IPR 2012). pp. 1–6 (Jul 2012)
8. Roweis, S.: EM algorithms for PCA and SPCA. In: Proceedings of the 1997 conference on Advances in neural information processing systems 10. pp. 626–632. NIPS '97, MIT Press, Cambridge, MA, USA (1998)
9. Russakoff, D.B., Tomasi, C., Rohlfing, T., Maurer, C.R.: Image similarity using mutual information of regions. In: Pajdla, T., Matas, J. (eds.) Computer Vision - ECCV 2004, vol. 3023, pp. 596–607. Springer Berlin Heidelberg, Berlin, Heidelberg (2004)
10. Simmons, A., Tofts, P.S., Barker, G.J., Arridge, S.R.: Sources of intensity nonuniformity in spin echo images at 1.5 t. Magnetic Resonance in Medicine 32(1), 121–128 (Jul 1994)
11. Studholme, Hill, D., Hawkes, D.J.: An overlap invariant entropy measure of 3D medical image alignment . Pattern Recognition 32(1), 71–86 (1999)
12. Viola, P., Wells, W.M.: Alignment by maximization of mutual information. In: Fifth International Conference on Computer Vision, 1995. Proceedings. pp. 16–23. IEEE (Jun 1995)
13. Yang, C., Jiang, T., Wang, J., Zheng, L.: A neighborhood incorporated method in image registration. Image Rochester NY pp. 244–251 (2006)
14. Zitová, B., Flusser, J.: Image registration methods: a survey. Image and Vision Computing 21(11), 977–1000 (Oct 2003)